Survey Design for Small Autonomous Ground-Based Telescopes To Detect Uncontrolled/Debris GEO Objects

Akhter Mahmud Nafi, David Geller
Mechanical and Aerospace Engineering, Utah State University, Logan, UT, USA

ABSTRACT

Innovative surveys of uncontrolled GEO debris objects are designed for a small autonomous ground-based telescope. The key innovation is that the survey designs are based on the known astrodynamics of uncontrolled GEO objects (e.g. due lunar/solar perturbations) combined with the current concentration of catalogued uncontrolled/debris GEO objects. The more practical matters of solar phase angle, lunar/galactic center proximity, and telescope slew rate are considered, and used to develop surveys that maximize the number of observed near-GEO uncontrolled/debris objects and enhance the Space Situational Awareness (SSA) of the GEO belt region.

1. INTRODUCTION

Space debris detection, catalogue updating, and understanding long term GEO object behavior is imperative for future space missions. Survey campaigns conducted by NASA and ESA indicate that man-made Earth orbiting debris is increasing especially in near Geosynchronous orbit (GEO) [13, 9]. Furthermore at least five breakups have been confirmed in this regime [8]. Debris created from recent breakups and older uncooperative satellites and rocket bodies in this regime pose a threat to active payloads. Ground-based Electro optical (EO) sensors are the cost effective way to detect objects at GEO altitude. Therefore, it is important to design effective surveys to detect objects using ground-based observatories. The main purpose of this paper is to design and simulate multiple effective surveys for a small autonomous ground-based observatory specifically for near-GEO uncontrolled/debris objects. In this research uncontrolled/debris GEO resident space objects (RSOs) are defined as near GEO objects with inclinations greater than 2°.

The objectives of this research are threefold: 1) develop an efficient ground-based optical survey strategy that utilizes the astrodynamics of the GEO environment and the known concentrations of current uncontrolled GEO objects to maximize the coverage of GEO space debris while ensuring good visibility/lighting and good information content; 2) test and assess the merit of the new survey strategy through simulation using metrics which include number of unique objects detected, required telescope movement, and GEO belt coverage; and 3) test and assess the merit of the new survey strategy by utilizing USU's Space Situational Awareness Telescope for Astrodynamics Research (USU-STAR) to validate simulation results. The first two objectives are addressed in this paper.

In previous work, ground-based GEO surveys have been designed and implemented based on the solar phase angle [9, 10, 1], coverage of the GEO regime [11, 4], state information [3], combining visibility, coverage and state information [6], and treating the survey design as an optimization problem [5]. Sharma et al. [12] selected the most congested locations in GEO belt known as Pinch Points to develop a survey strategy using a space-based sensor. The aspects of a Pinch Point survey using a ground-based observatory have also been analyzed [7].

This research will use the information from current TLE catalog and the system information associated with the USU-STAR telescope (e.g. slew rates, field of view, etc.) to design surveys. Four other key factors are taken into account including (1) the concentration/distribution of catalogued uncontrolled GEO objects, (2) solar phase angle, (3) proximity of the moon, and (4) the proximity of the galactic center to the observed GEO object. Because of the nature of the GEO orbit, uncatalogued/uncorrelated debris will mimic the behavior of the cataloged uncontrolled objects and thus will also be observed. Further, ensuring a good solar phase angle will ensure object detection, and sufficient angular distance from the moon, as well as the galactic center, will ensure a saturation-free and star-crowd-free image. The surveys designed in this paper will be based on a performance index consisting of the four key factors stated above. Comparison of the surveys will be made on the number of unique objects detected, the angle between two consecutive slewing directions of the telescope, and the potential state information gathered from the survey. Future work will provide quantitative state information gathered from each survey.

2. APPROACH

When a space object becomes a debris object (i.e., uncontrolled), the orbital inclination of the GEO debris object increases from 0 degrees to 15 degrees and then decreases back to 0 degrees over a 53 year period as a result of lunar-solar and geopotential perturbation [14]. A consequence of this phenomena is that GEO space objects that were incapacitated 26.5 years ago are currently in a near 15 degree inclination orbit. Over the subsequent 26.5 years these objects return to a near 0 degree inclination orbit, the same orbit where our most valuable GEO assets reside. Fig. 1 shows the GEO object distribution in right ascension of the ascending node (RAAN) and inclination. A noticeable change after only 5 years shows that these debris objects will eventually return to orbits with 0 degree inclination. The fact that uncontrolled objects tend to group according to the RAAN- inclination pattern shown in Fig. 1 will be the first key element in this survey design.

Next key element, and the impetus for this work, is based on the idea of a "Pinch Point" survey [12] for space-based observatories, which is in turn based on GEO object concentrations in right ascension and declination (RA-DEC) space over a 24 hour period. In the geocentric frame the zero declination region is more concentrated than any other declination. Some areas are more crowded than others primarily due to the passing of uncontrolled satellites through the region over 24 hour period, i.e., the most concentrated pinch point regions are produced by uncontrolled objects travel through their ascending nodes (Region 1) and their descending nodes (Region 2). Fig. 2 gives a visualization of the number of satellites passing through RA-DEC space over a 24 hour period. Most of the controlled satellites follow the geocentric declination close to 0°. Regions near RA 70° and RA -250° are the most densely populated relative to rest of the right ascension space.

Fig. 2 shows the concentration of all GEO catalogued object. In this work, only uncontrolled catalogued object concentrations are considered. Fig. 3 shows the concentrations of uncontrolled/debris object in RA-DEC frame for the evening of July 7, 2017. Multiple survey designs are presented based on the concentration of known uncontrolled GEO debris and also ensure that the surveys are performed in favorable observation conditions. By following the highest concentration regions of uncontrolled catalogued objects, it is hypothesized that this will also maximize the number of detected uncontrolled uncatalogued/uncorrelated object detections.

Future work includes developing a metric to measure the total state information of the designed surveys, and validating all results using the USU-STAR.

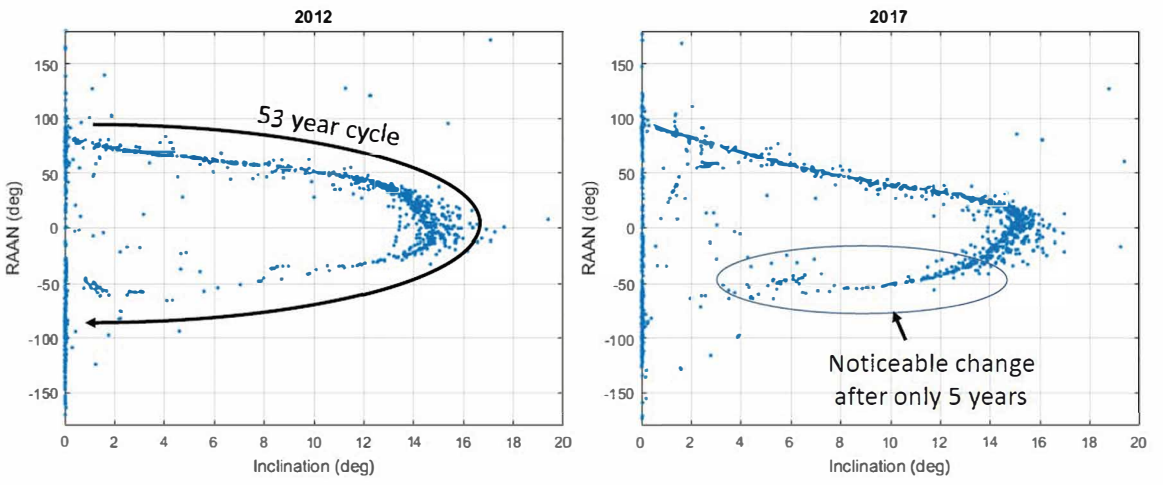

Fig. 1: RAAN-inclination of uncontrolled GEO objects, 2012 (right), 2017 (left)

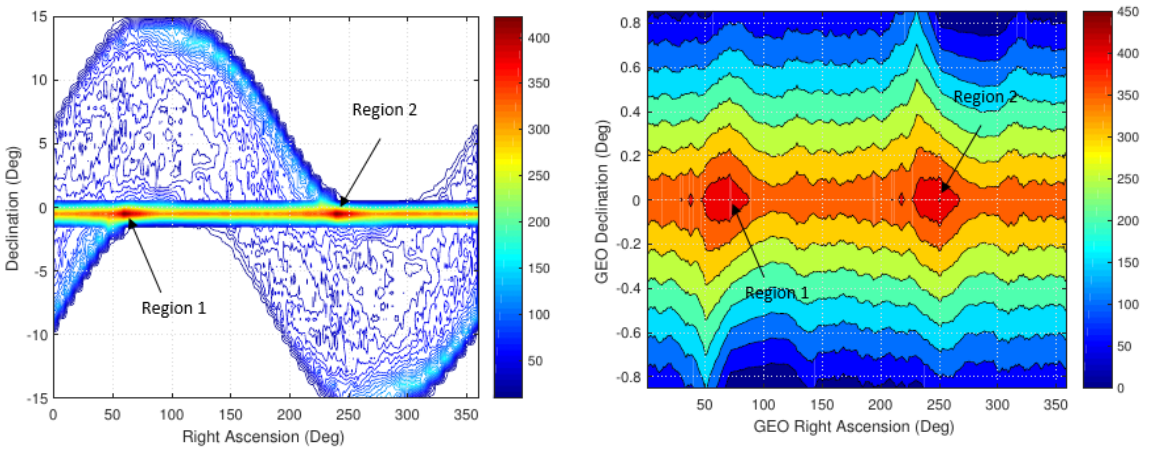

(a) Geocentric right ascension and declination frame

(b) Geocentric right ascension and declination frame

Fig. 2: Satellite concentration in the geosynchronous belt over a 24 hour period, 11 Nov 2017

3. PROBLEM SETUP

All survey designs will be applied to a catalogue of uncontrolled GEO objects, in this research uncontrolled GEO objects are defined as near GEO objects with inclinations (i) greater than 2° and semi-major axes (a) between 40000 km and 44000 km. For the survey designs the uncontrolled/debris orbital set $\mathcal{S}$ defined as

$$\mathcal{S} = \{a \in [40000 \text{ km}, 44000 \text{ km}] \cap i > 2^\circ\} \tag{1}$$

The catalogued uncontrolled/debris RSOs in set $\mathcal{S}$ are then given a unique identification (id) based on their order in the TLE catalogue.

The observation period for ground-based optical telescope varies widely from season to season. To see the effect of observation time for two different seasons, surveys are designed for both summer (17 July, 2018) and winter (11 November, 2017). The observation time is set from sunset to sunrise with astronomical twilight taken into account. This provided 10 hrs and 50 mins of observation time for the evening of 11 November 2017 and only 5hrs of observation time for evening of 17 July 2018. For each survey, summer and winter results will be represented by S and W respectively, e.g. Survey 1W, Survey 3S etc.

Publicly available RSO data from space-track.org is used to propagate uncontrolled GEO RSOs for both dates. $\mathcal{S}$ includes 860 RSOs in winter (only 296 can be viewed from Bear Lake, UT) and 890 objects in summer survey (only 249 can be viewed from Bear Lake, UT). System parameters consist of the location of the observatory, telescope, camera specification and observation time interval. Surveys in this paper are designed based on the system parameters of USU-STAR telescope installed near Bear Lake, Utah, but the approach can be applied to any observatory. The system parameters for all surveys are shown in Table. 1.

With the exception of the Pinch Point survey, all surveys will select various high concentration locations in the sky and will not track a single point in RA-DEC space and significant slewing of the telescope may be required. Thus it is important for the survey design to ensure the telescope has enough time to reach a given pointing direction. A single performance metric, $\Delta\theta$, is introduced to score the telescope movement of the entire survey, where $\Delta\theta_i$ is the angle between the telescope pointing direction l_{t_i} at time t_i, and the telescope pointing direction at previous time $l_{t_{i-1}}$ in the local azimuth-elevation frame.

$$\Delta\theta_i = \cos^{-1}(l_{t_i}.l_{t_{i-1}}) \tag{2}$$

The average $\Delta\theta$ and the standard deviation of $\Delta\theta$ of every survey will indicate the feasibility of the implementation based on the slewing capability of the telescope. Zero $\Delta\theta$ means the telescope is tracking the same point in local azimuth-elevation frame. A large value of $\Delta\theta$ does not guarantee object detection as the telescope may not have

Parameters	
Latitude of the observatory	41.9°
Longitude of the observatory	-111.42°
Altitude of the observatory	1.98 Km
Aperture Diameter	25 cm
Field of View (FOV)	$1.28 \times 1.28°$
Size of Frame	4096×4096
Pixel size	9 μm
Imaging mode	Earth tracking mode
Time between measurements	20 sec (Survey 1), 30 sec (Survey 2-7)
Exposure time	5 sec
Read out time	5 sec
Time for Slewing	20 sec

Table 1: System parameters for survey design

enough time to slew to the intended RA-DEC at the desired time. As will be seen, the Pinch Point survey (Survey 1), requires very little telescope slewing. The time between measurements is thus selected to be only 20 sec.

For the other surveys, the time between each observation is selected as 30 sec. All surveys assume 5°/sec slew rate, camera exposure times of 5 sec, camera readout of 5 sec, and the remaining 20 sec for slewing. Thus, the maximum $\Delta\theta_i$ is considered to be 100°, since if $\Delta\theta_i$ >100 °, the telescope may not have enough time to reach the commanded RA-DEC.

In addition to $\Delta\theta$, four other key angles related to survey performance will be utilized: 1) the solar phase angle of the center of the FOV (ϕ) is a measure of visibility of an RSO, the elevation of the center of the FOV(λ) indicates whether or not the RSO is above horizon, the angle between moon and the center of the FOV (ξ) indicates the level of moonlight interference, and the angle between the galactic center and the center of the FOV (ψ) is an indication of the level of background star concentration. These four angles and $\Delta\theta$ will be presented for each survey. A well-designed survey should avoid the galactic plane by at least 10° [1] and the moon by 15° (from practical survey experience).

4. SURVEY DESIGN

4.1 SURVEY DESIGN 1 – PINCH POINT TRACKING (PPT)

The main idea behind this first survey strategy is to track the Pinch Points with the highest satellite concentration of uncontrolled GEO objects shown in Fig. 3. By following the highest concentration regions, it is hypothesized that more uncatalogued uncontrolled satellites and uncatalogued debris can be detected. In Fig. 3 it can be seen that there are several high concentration regions, instead of only two as discussed in Section 2. Among the several Pinch Points, -4.5° DEC, 14.5° RA and -14.7° DEC, 253° RA are the two Pinch Points selected for Survey 1.

However, Fig. 4 shows that the Pinch Points may not be above the horizon during the night from the perspective of the specific observatory, or may have a very small time period before setting below the horizon, or may have poor solar phase angles. In the first case it is impossible to conduct any survey. For the second case, the total observation time is not utilized efficiently and in the third case, the objects may not be visible. The elevation of the Pinch Points also depends on the season of the year.

As shown in Fig. 4(a) Pinch Point 2 is not visible from the observatory. Thus Survey 1W focused entirely on Pinch Point 1. Pinch Point 1 is above 15 ° elevation for 7 hrs. Fig. 4(b) shows that Pinch Point 1 is visible for only a very short period of time. Thus, Survey 1S focused on Pinch Point 2 and it is visible for 2 hrs 30 mins.

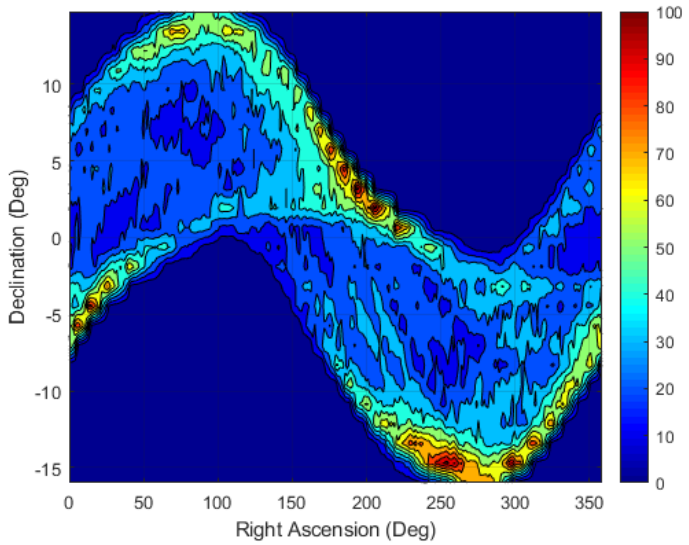

Fig. 3: Uncontrolled satellite concentration in the geosynchronous belt over entire observation hr period, 2017

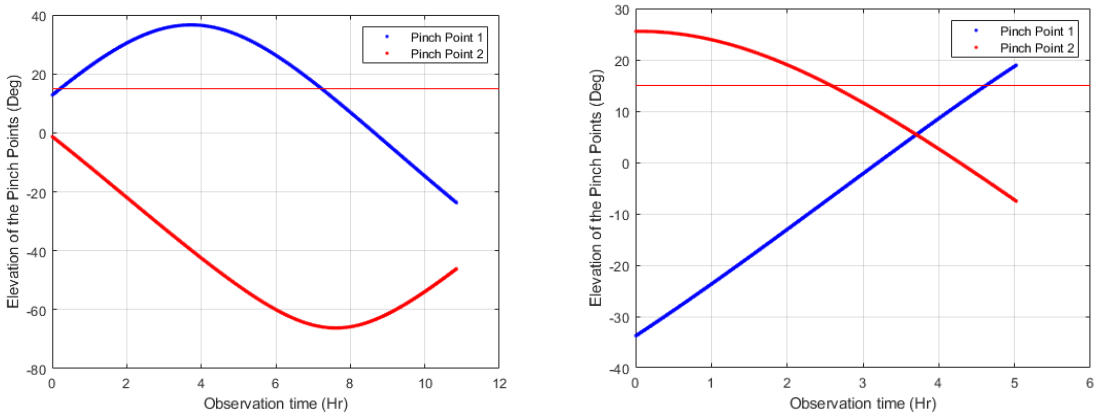

(a) Pinch Point elevation 11 November, 2017

(b) Pinch Point elevation 17 July, 2018

Fig. 4: Pinch Point elevation

4.2 SURVEY DESIGN 2 – MODIFIED PINCH POINT TRACKING (MPPT)

In Survey 1, the Pinch Point may not be visible from the observatory throughout the night, the solar phase angle may not be favorable, or the moon or galactic center may be very close to the field of view. Survey 2 is designed to overcome these challenges by providing flexibility to move away from the Pinch Point when the above unfavorable conditions exist.

For Survey 2, and all subsequent survey designs, the following constraints are enforced:

$$\text{solar phase angle} \qquad \phi(\alpha_{FOV}, \delta_{FOV}, t) > 90^\circ \tag{3}$$

$$\text{local elevation} \qquad \lambda(\alpha_{FOV}, \delta_{FOV}, t) > 15^\circ \tag{4}$$

$$\text{lunar angular displacement} \qquad \xi(\alpha_{FOV}, \delta_{FOV}, t) > 20^\circ \tag{5}$$

$$\text{galactic center angular displacement} \qquad \psi(\alpha_{FOV}, \delta_{FOV}, t) > 10^\circ \tag{6}$$

Where α_{FOV} and δ_{FOV} represents the center of the telescope FOV in the RA-DEC frame.

Survey 2 first creates a grid in RA-DEC space and populated by the number n of uncontrolled catalogued RSOs that pass through each cell throughout the entire observation period. Each cell of the grid has the same size as the FOV of the ground-based telescope. ϕ, λ, ξ, and ψ are computed at each observation time, t_i, for each cell in the grid. Then, each cell is assigned 4 weights, $W_{\phi,i}, W_{\lambda,i}, W_{\xi,i}$, and $W_{\psi,i}$, which are equal to 100 if the constraint is satisfied, or zero if not. Finally, a performance index J_i is computed and assigned to each cell in the grid at each observation time, t_i .

$$J_i = n \times W_{\phi,i} \times W_{\lambda,i} \times W_{\xi,i} \times W_{\psi,i} \tag{7}$$

The survey is designed by selecting the cell with the highest performance index at each time step, i.e., the cell with the highest value of J_i. The survey will always image the RA-DEC location with the largest number of RSOs subject to the constraints in Eqs. 3-6.

4.3 SURVEY DESIGN 3 – MAXIMIZE OBJECT OBSERVATIONS (MOO)

For Survey 1 and 2 a single grid in RA-DEC space was created where each cell representing a potential telescope pointing direction was populated with the number of objects passing through that cell over an entire observation period utilizing a GEO catalogue of uncontrolled objects. For Survey 2, each cell was also weighted according the constraints that had been satisfied at each time t_i.

For Survey 3, a grid is created at each possible observation time t_i, and the cells are populated by the number of objects that occupy that cell at time t_i. The cells are then weighted by the performance index J_i in Eq 7. In effect, this creates a performance grid in RA-DEC space at each time t_i. If multiple cells of the grid satisfy all the survey requirements, then the performance index only depends on the number of RSOs stored in the cell. If multiple cells have equal performance indices, the algorithm will select the cell that is closest to the cell associated with the previous observation.

4.4 SURVEY DESIGN 4 – RANDOM RA-DEC SELECTION (RRDS)

As will be seen, one of the drawbacks of Survey 3 is that some of the cells in the RA-DEC space are tracked repeatedly because these cells nearly always have the highest performance index. Survey 4 is designed to overcome this issue. In Survey 4, the grid cells at each time t_i will be populated in the same manner as in Survey 3, and each cell at each time will be scored using Eq 7. However, instead of selecting the cell with the highest performance index (as in Survey 3), Survey 4 will randomly select from all the cells with performance index J_i greater than zero in the grid. Performance index J_i greater than zero ensures there will be at least 1 satellites in the FOV at that time step. Because of the random selection, this survey method will not track the same group of satellites repeatedly.

4.5 SURVEY DESIGN 5 – WEIGHTED OBJECT OBSERVATION (WOO)

Survey 4 eliminated the Survey 3 problem of repeatedly tracking the same groups of objects, but the random selection of RA-DEC locations results in very large $\Delta\theta_i$ from one observation to the next. Further, as will be seen, Survey 4 did not do well in the area of detecting unique RSOs at least 3 times, required for IOD.

Survey 5 represents a second attempt to improve Survey 3 (without selecting random pointing directions) by implementing a new constraint such that whenever any cell contains a RSO that has been already tracked more than 4 times, the performance index J_i is down-weighted by a factor of 20. This will force the survey to go to another location after the down-weighting occurs rather than repeatedly tracking the same groups of satellites (or same RA-DEC). Dividing by 20 ensures the telescope will again track the group or individual RSO that has already been tracked 4 times only if there are no other individual favorable RSOs in the whole grid. The down-weight method ensures that even one previously undetected RSO in a different cell will have a greater performance index than the cell having a group of RSOs tracked at least 4 times.

4.6 SURVEY DESIGN 6 – RANDOM OBSERVATION TIME SELECTION (ROTS)

One of the drawbacks of Survey 5 is that the survey selects the cell with the highest performance index in chronological order. This results in 4 back-to-back observations of the same object, and will potentially result in very poor state information content. To overcome this problem, Survey 6 observations are selected randomly in time until a full night of observations are scheduled. Groups of RSOs that are observed four times are still down-weighed by a factor of 20 after each observation, but the observations will be more spaced out over the night in a random manner resulting in potentially higher state information content. Thus, in Survey 6 a group of RSOs will not be tracked repeatedly as

Survey 3 and individual RSO detection will be more spaced out in time than Survey 5 as down-weighting and random observation time selection is occurring simultaneously.

4.7 SURVEY DESIGN 7 – GUARANTEED INITIAL ORBIT DETERMINATION (GIOD)

Initial orbit determination (IOD) of an RSO requires at least 3 sets of angle measurements. For a GEO RSO, the time difference between each measurement should be reasonably large due to the geometry of the orbit [2]. Survey 7 is designed to ensure at least 3 observations (3 sets of angle measurements) with a specified time interval between measurements for each RSO. Initially an $S \times K$ matrix Q is created, where S is the number of satellites and K is the total number of observation times. If an RSO satisfies all the observation constraints in Eqs. 3-6 at any observation time, a value of 1 is stored at that element of the matrix, otherwise a value of 0 is stored in that element.

Next, satellites are prioritized based on their availability for observation in the entire observation time. RSOs with lower availability get higher priority. Some RSOs have a 1 in every column of the matrix Q which indicates the RSO is visible with favorable observation condition for the entire night, and the priority of these RSOs will be less compared to the other RSOs having fewer ones in the matrix Q. High priority satellites will be assigned time slots first to collect 3 images 20 min apart, then the time slots will be allocated to lower priority satellites.

Using this strategy not all RSOs are selected for observation. Only those that can be detected at least 3 times separated by a 20 min interval are selected for the survey. That means an RSO has to satisfy all the observation constraints for at least 60 mins in the entire night to be eligible for the survey.

5. RESULTS

Data and plots for each survey are generated automatically showing the telescope pointing directions in the RA-DEC frame and the local azimuth-elevation frame. In addition, the time histories of $\Delta\theta_i$, the observed satellite id, the number of objects in each image, and the accumulated number of observed RSOs is generated. In this section, only the results for the most promising surveys are presented.

The reader is reminded that although 860 catalogued uncontrolled GEO RSOs are in set $\mathcal{S}$ in winter and 890 catalogued uncontrolled GEO objects are in set $\mathcal{S}$ in summer, not all of them are detectable since their elevation may not be above 15° for any part of observation period from Bear lake, UT. The maximum number of catalogued objects that can be detected in the winter surveys is 296, (Bear Lake, UT, 11 November 2017), and maximum number of objects that can be detected in summer surveys is 249 (Bear Lake, UT, 17 July 2018).

5.1 Survey 2W (Winter, 11 Nov 2017)

Unlike Survey 1W, Survey 2W was forced to meet all the user defined constraints. Fig. 5 shows the time history of the pointing direction of the telescope in the RA-DEC coordinates and local azimuth-elevation coordinates. Fig. 5(c) and Fig. 5(d) show that other than for a brief period at the beginning, the survey is tracking a single point in RA-DEC space, and as soon as the point does not have favorable observation conditions (e.g. the cell that contained the largest number of GEO objects is below the horizon), the survey looks for the next best cell that satisfies all the criteria stated above. Thus, the survey switches to higher RA-DEC and eventually settles for 70° RA and 14.08° DEC. Fig. 5(e) shows that Survey 2W scans the sky from east to west for more than 6 hrs of observation time and then south to west through the remaining observation time (azimuth is measured counterclockwise from east).

In this survey ϕ is always greater than 130°, ξ is greater than 70°, and ψ is greater than 90°, which ensures good observation conditions throughout the entire survey. The $\Delta\theta_i$ time history in Fig. 6(a) shows that the telescope slewing requirement is well bellow the 100° constraint throughout the entire observation time. The mean slew angle, $\mu_{\Delta\theta} = 0.19°$, and the mean plus 2σ slew angle, $\mu_{\Delta\theta} + 2\sigma_{\Delta\theta} = 3.07°$ are small and ensure that Survey 2W can be accomplished without excessive slewing.

Fig. 6(d) shows that a total of 83 unique objects are detected and 80 of them are detected at least 3 times (at least 3 observations are required for angles only initial orbit determination). The 83 unique catalogued RSOs are imaged a total of 801 times. However, 708 image frames did not contain any satellites and a maximum 4 satellites are detected in a single image frame.

5.2 Survey 2S (Summer, 17 July 2018)

This survey scans generally from south to west and then eastern parts of the sky, and ϕ is greater than 90°, ξ is greater than 60°, and ψ is greater than 10 °, which ensure good observation conditions throughout the entire survey. The mean

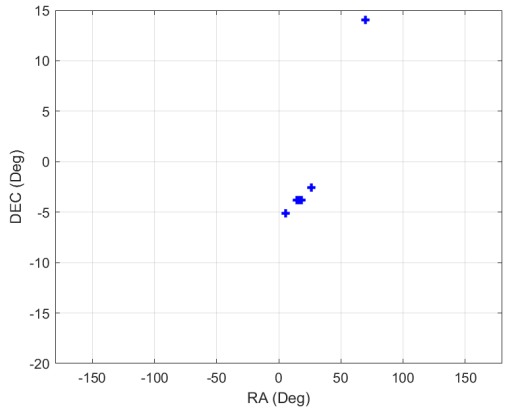

(a) Survey in geocentric right ascension and declination frame

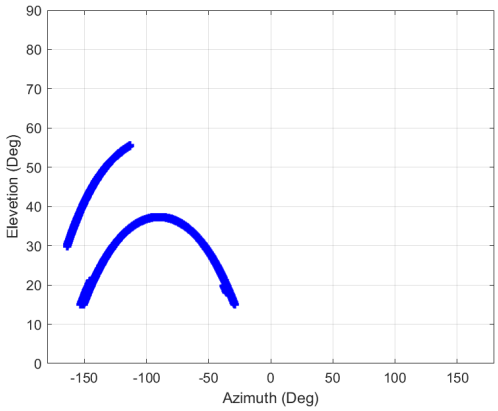

(b) Survey in geocentric azimuth and elevation frame

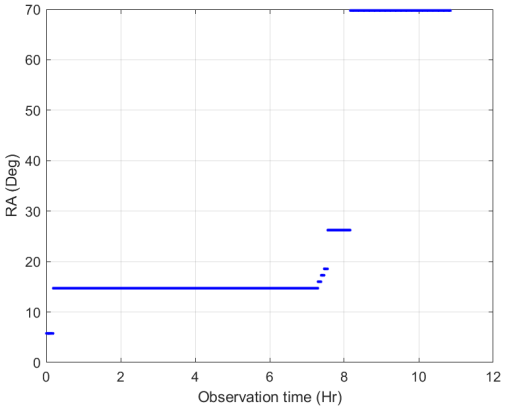

(c) RA time history

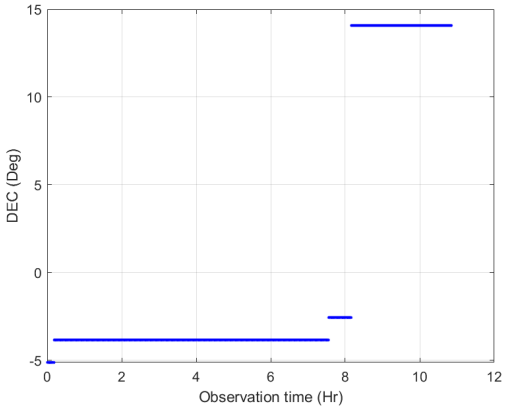

(d) DEC time history

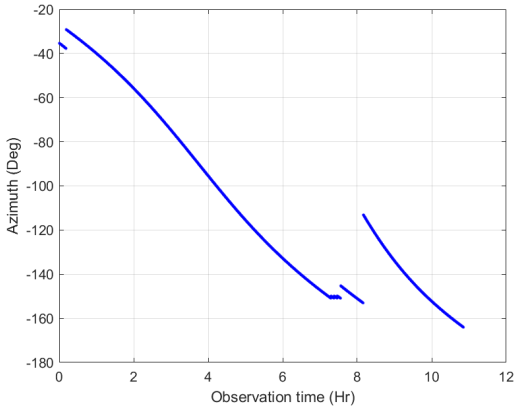

(e) Azimuth time history

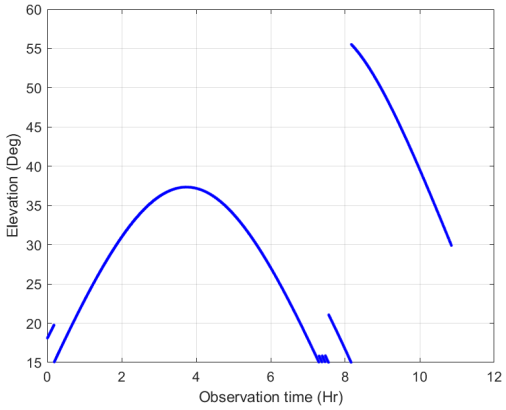

(f) Elevation time history

Fig. 5: Telescope pointing, Survey 2W (Winter, 11 Nov 2017)

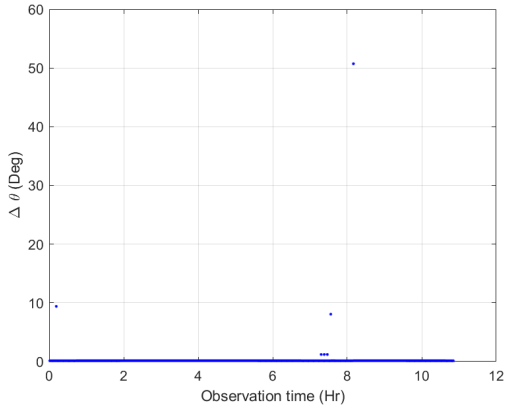

(a) $\Delta\theta$ time history

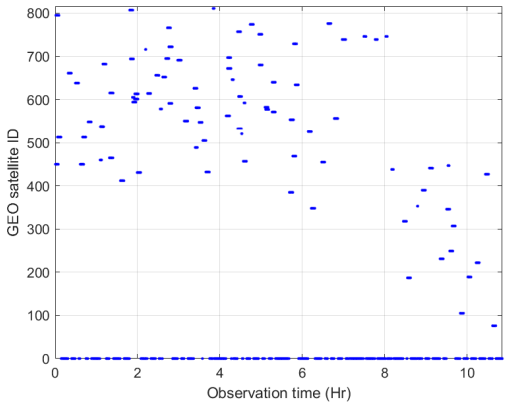

(b) GEO satellites detection time history

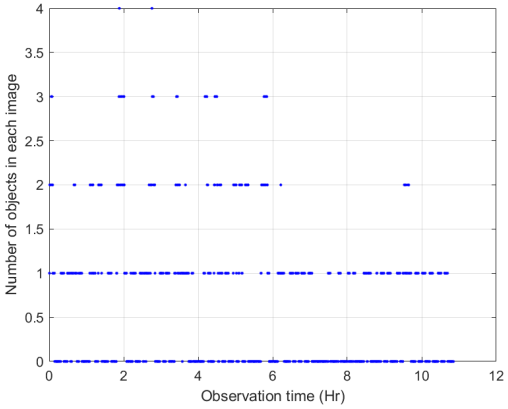

(c) Number of satellites in each image

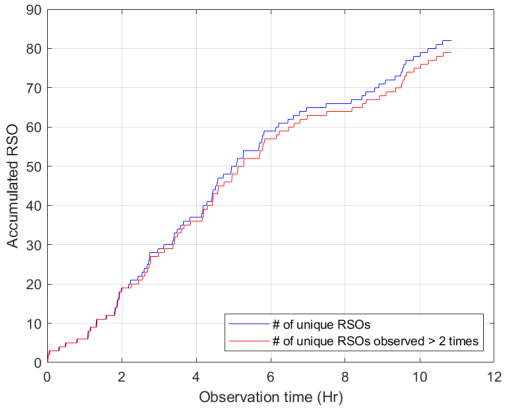

(d) Accumulation of RSO time history

Fig. 6: RSO data, Survey 2W (Winter, 11 Nov 2017)

slew angle and mean plus 2σ slew angle are $\mu_{\Delta\theta} = 0.36^\circ$ and $\mu_{\Delta\theta} + 2\sigma_{\Delta\theta}$ =6.07°, respectively, and show that telescope slewing times are well within the bounds.

The maximum number of RSOs in an image frame is 4, and most of the detected RSOs are tracked 10 or 11 times. A total of 37 unique objects were detected and 34 of them were detected at least three times. The 37 unique catalogued RSOs were imaged a total of 429 times.

5.3 Survey 3W (Winter, 11 Nov 2017)

The results for Survey 3W are shown in Fig. 7-8. Fig. 7(a) shows that Survey 3W scans through the entire visible GEO belt area in RA-DEC space. Fig. 7(c) illustrates some linear tracking features in RA space. This indicates that the survey is tracking on the order of 20 groups of RSOs through the entire observation period. Fig. 7(e) shows that the survey is generally slewing back and forth from east to south at the beginning of the survey and back and forth from south to west at the end of the survey. The elevation is never below 15° as shown in Fig. 7(b), and ϕ is greater than 90°, ξ is greater than 20°, and ψ is greater than 40° throughout the entire survey. The mean slew angle, $\mu_{\Delta\theta}$= 22.91°, and the mean plus 2σ slew angle, $\mu_{\Delta\theta} + 2\sigma_{\Delta\theta}$= 77.42° show that there will be more slewing activity than previous surveys, but the slewing is within the maximum capability of the telescope.

Fig. 8(b) shows the GEO satellites detection time history and Fig. 8(d) shows the accumulated RSO data over time. Both figures confirm the repeating characteristics of the survey. An abundance of horizontal streaks in Fig. 8(b) clearly indicates that some RSOs are tracked repeatedly, and in some cases the RSOs are tracked more than 150 times. Fig. 8(c) shows that the maximum number of RSO in a single image is 5. Survey 3W has at least 2 RSOs in every image compared to 708 images with zero satellites in Survey 2W. One of the goals of the newly designed survey was to maximize the number of object observations, which is surely visible in Fig. 8(b).

Fig. 8(d) shows that a total of 206 unique RSOs are detected, 158 of them at least 3 times, as compared to Survey 2W where 83 unique RSOs were detected, 80 of them at least 3 times. The 206 unique catalogued RSOs are imaged a total of 3833 times, while the 83 unique RSOs in Survey 2W are imaged only 801 times. In this sense, Survey 3W acheived the goal to max the number of objects observations.

5.4 Survey 3S (Summer, 17 July 2018)

Survey 3S shows similar characteristics as Survey 3W. Repeated RSO tracking is again evident where approximately 15 groups of RSOs are tracked repeatedly. The elevation is never below 15°, ϕ is always greater than 90°, ξ is greater than 20°, and ψ is greater than 10° which ensure good observation conditions throughout the entire survey. The mean slew angle, $\mu_{\Delta\theta}$= 23.69°, and the mean plus 2σ slew angle, $\mu_{\Delta\theta} + 2\sigma_{\Delta\theta}$= 79.25° show that telescope slewing is well within the bounds.

For this survey the maximum number of RSO in image frame is 4. A total of only 126 unique RSOs are detected, 95 of them at least 3 times, as compared to Survey 2S where 37 unique RSOs were detected, 34 of them at least 3 times. So, in this sense Survey 3S increased the number of unique RSOs. The 126 unique uncontrolled catalogued RSOs are imaged 1742 times, while the 37 unique RSOs in Survey 2S are imaged only 429 times. In this sense, Survey 3S also achieved the goal to maximize the number of object observations.

5.5 Survey 6W (Winter, 11 Nov 2017)

The results for Survey 6W are shown in Fig. 9-10. Fig. 9(a) shows that the survey scans through the visible GEO belt in RA-DEC space. Fig. 9(e) and Fig. 9(f) shows that the azimuth and the elevation angles of the pointing directions are scattered throughout the survey. Fig. 9(f) illustrates that the elevation is always above 15°.

For this survey ϕ is always greater than 90°, ξ is greater than 20°, and ψ is greater than 40°. The mean slew angle, $\mu_{\Delta\theta}$ was 35.84° and the system will be able to slew to most of the objects in the required 20 sec as the mean plus 2σ slew angle, $\mu_{\Delta\theta} + 2\sigma_{\Delta\theta}$ is 93.97° (<100 °).

Fig. 10(b) shows how the GEO RSOs detections are uniformly distributed as a function of observation time. Fig. 10(c) shows that the maximum number of satellite in the image frame is 4. Some RSOs are tracked more than 50 times, but most of the RSOs are detected between 4 to 10 times. Fig. 10(d) shows that the total number of unique RSOs detected is 295. The number of RSOs detected more than 3 times is 294. The 295 unique uncontrolled catalogued RSOs are imaged 3219 times.

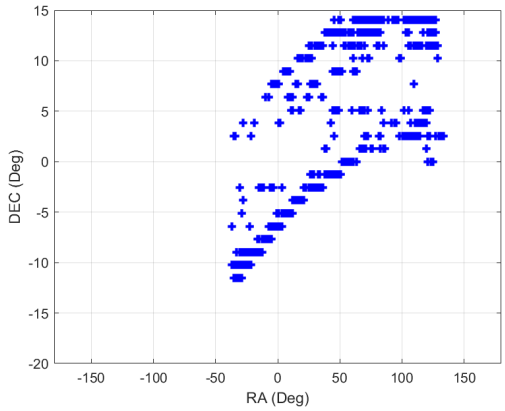

(a) Survey in geocentric right ascension and declination frame

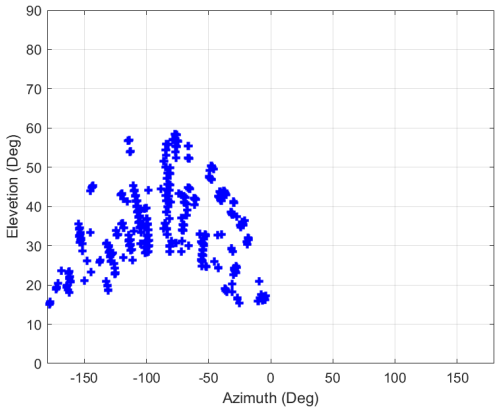

(b) Survey in geocentric azimuth and elevation frame

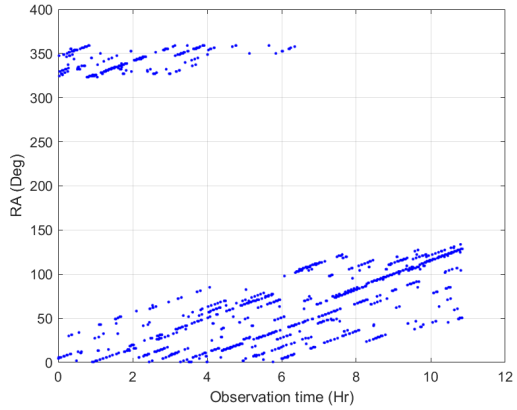

(c) RA time history

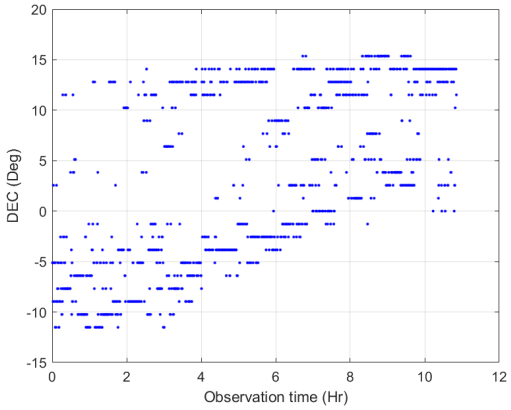

(d) DEC time history

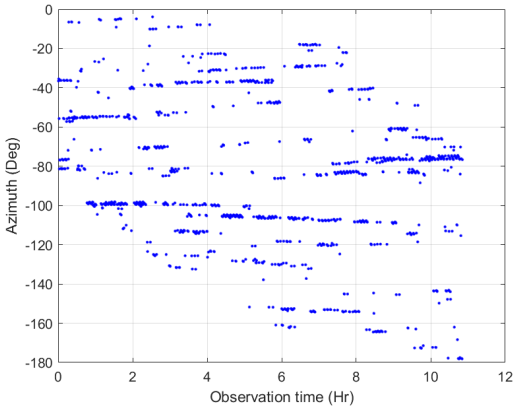

(e) Azimuth time history

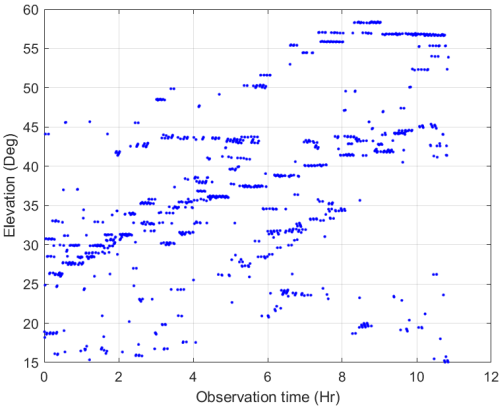

(f) Elevation time history

Fig. 7: Telescope pointing, Survey 3W (Winter, 11 Nov,2017)

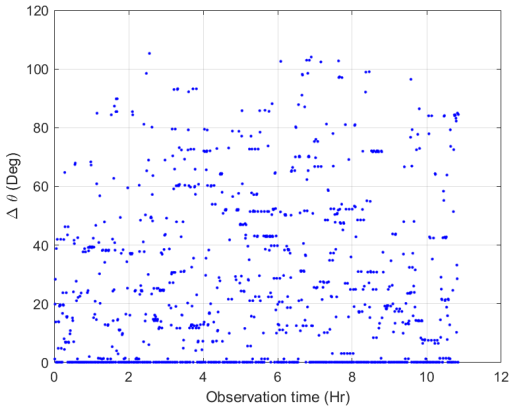

(a) $\Delta\theta$ time history

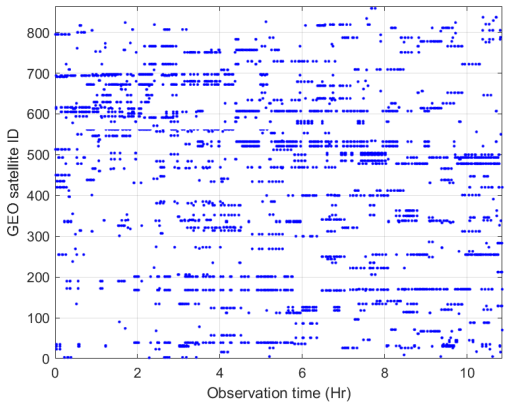

(b) GEO satellites detection time history

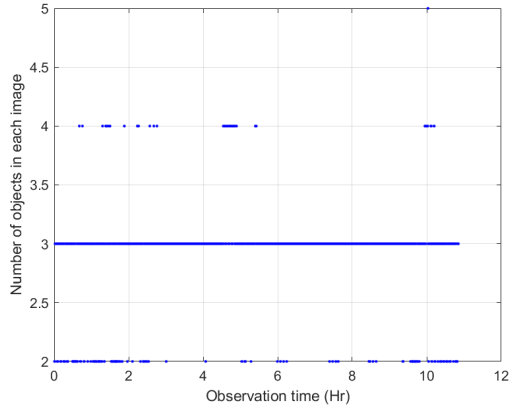

(c) Number of satellites in each image

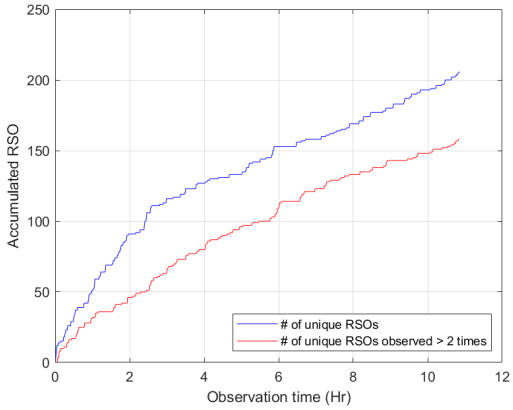

(d) Accumulation of RSO time history

Fig. 8: RSO data, Survey 3W (Winter, 11 Nov,2017)

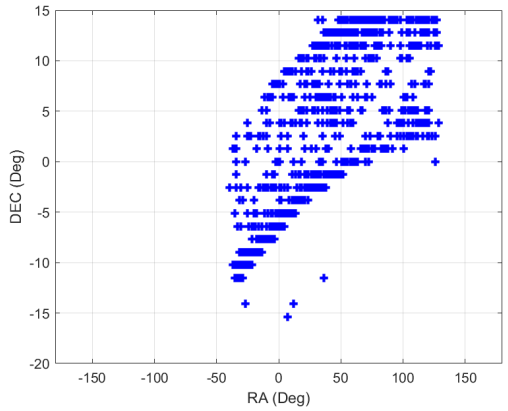

(a) Survey in geocentric right ascension and declination frame

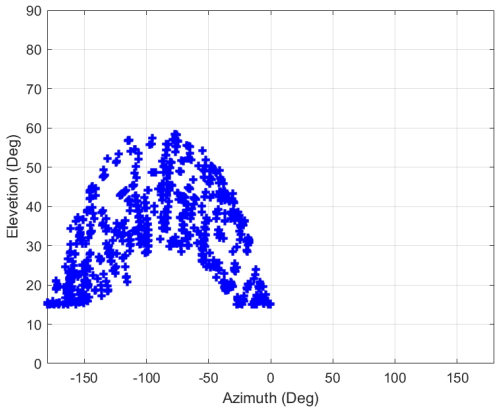

(b) Survey in geocentric azimuth and elevation frame

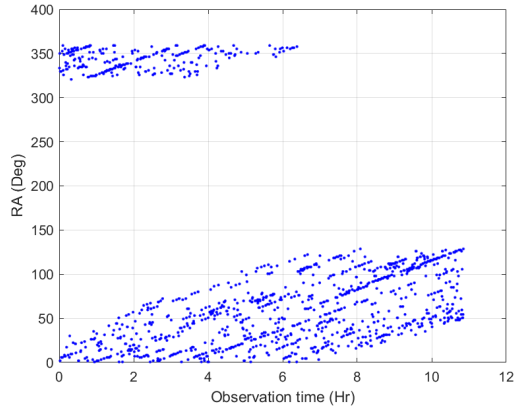

(c) RA time history

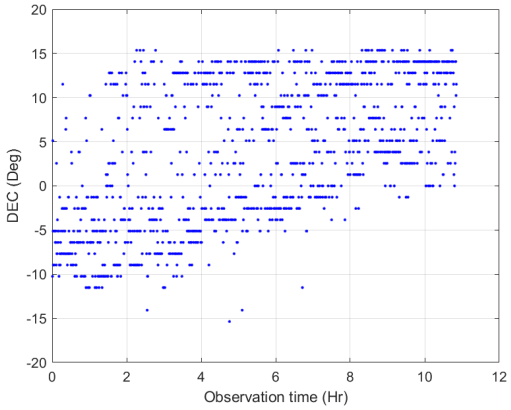

(d) DEC time history

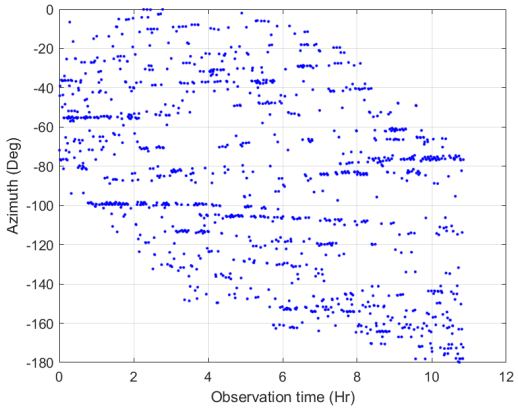

(e) Azimuth time history

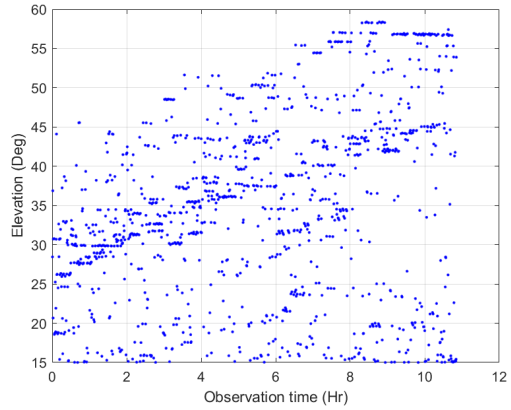

(f) Elevation time history

Fig. 9: Telescope pointing, Survey 6W (Winter, 11 Nov 2017)

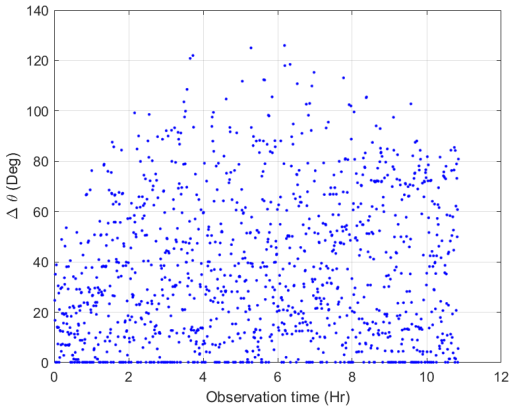

(a) $\Delta\theta$ time history

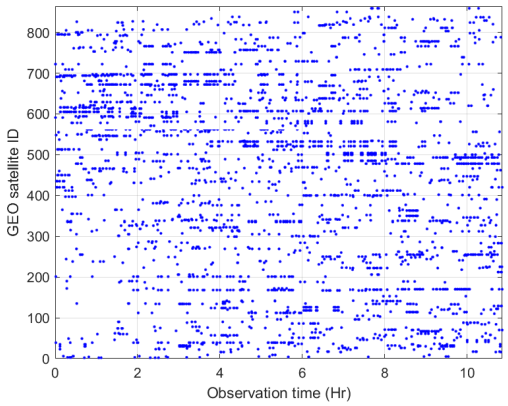

(b) GEO satellites detection time history

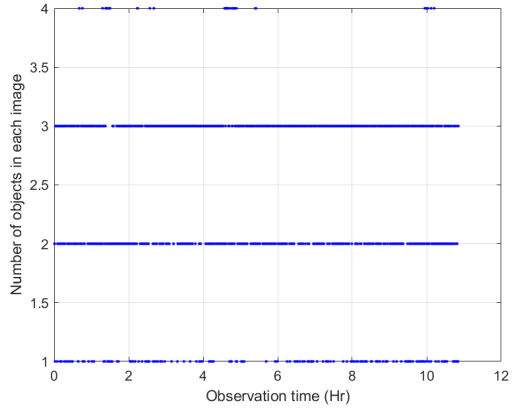

(c) Number of satellites in each image

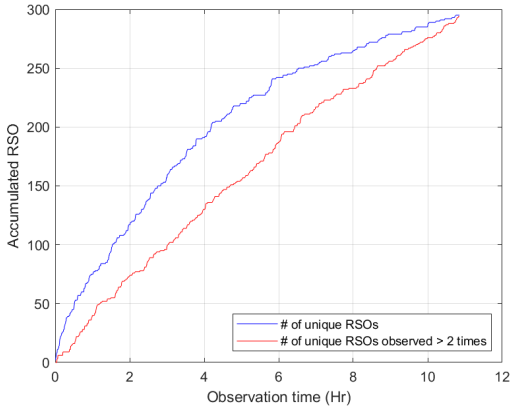

(d) Accumulation of RSO time history

Fig. 10: RSO data, Survey 6W (Winter, 11 Nov 2017)

5.6 Survey 6S (Summer, 17 July 2018)

The results for Survey 6S show similar trends. Most RSOs are tracked more than 3 times. A maximum 4 RSOs are detected in a single image, and here every image has at least 1 RSO. A total of 239 unique RSOs are detected and 230 of them are detected at least 3 times which is much higher than Survey 2S, Survey 3S, and slightly higher than 5S. The 239 unique catalogued RSOs are imaged 1235 times.

5.7 Survey 7W (Winter, 11 Nov 2017)

Fig. 11 shows that this survey scans through the visible GEO belt in RA-DEC space and the azimuth and the elevation angles of the telescope pointing direction are scattered throughout the survey and the elevation is always above 15°.

The survey has favorable viewing condition throughout the entire night ensured by the design. The mean slew angle $\mu_{\Delta\theta} = 27.21^\circ$ and the mean plus 2σ slew angle, $\mu_{\Delta\theta} + 2\sigma_{\Delta\theta} = 85.81^\circ$ is below the maximum slewing capacity of the telescope. The $\Delta\theta$ plot indicates that in some cases the slew requirement of the telescope will be very large ($> 100^\circ$). In those cases the telescope may not be able to point to the desired direction at that specific time.

A maximum 4 RSOs can be detected in a single image. The number of unique RSOs detected is 284, and all of them are detected at least 3 times. The 284 unique catalogued RSOs are imaged 1053 times.

5.8 Survey 7S (Summer, 17 July 2018)

Survey 7S shows similar trends, and detects 201 unique objects and 195 of them are detected at least 3 times. A maximum of 3 satellites are detected in a single image frame and the highest number of detection for single satellite is 9. The 201 unique uncontrolled catalogued RSOs are imaged 713 times.

6. SUMMARY AND CONCLUSIONS

Tables 2-3 and Fig. 13 summarize the results of all 7 surveys. Table 2 shows the results for the winter surveys and Table 3 shows the results for summer surveys. Fig. 13 provides a more graphical comparison of the results.

Survey 1 does not utilize the entire observation time due to the unavailability of the Pinch Point nor does it account for unfavorable observation conditions, and as expected the unique object detection is less than the other surveys.

Survey 2 attempts to remedy the problems of Survey 1, as it satisfies the observation constraints, and attempts to maximize the observation time. An increase in the number of unique objects detected reflects the improvement of Survey 2, but in winter only 83 unique objects are detected among 296 potential detectable objects and in summer only 37 unique objects are detected among 249 potential detectable objects. Survey 3 shows a large improvement over Surveys 1 and 2, detecting 206 and 126 unique objects in winter and summer surveys, respectively. However, there is room for improvement since it is seen that there is a issue with repeated detection of few groups of RSOs.

Surveys 4, 5, and 6 are designed to address that issue, and all of them improve upon Survey 3 in terms of number of unique objects detected. Survey 4 is able to detect 282 unique objects in the winter and 126 in the summer. Further, in Survey 4, 82.9% of the unique objects are detected at least 3 times in the winter and 58.1% in the summer. On the other hand Survey 5 and 6 show similarities in the number of objects detected. In the winter and summer, both surveys are able to detect almost all the detectable uncontrolled catalogued objects, but Survey 5 detects fewer unique objects than Survey 6, and fewer objects with at least three observations. The state information content of Survey 6 will also be better than Survey 5 as observations of an RSO for Survey 6 are more spaced out over the night. Survey 7, which ensures 20 min interval between 3 guaranteed observations, detects 95.9% of the observable uncontrolled catalogued catalogued objects in the winter, but the number drops in the summer to only 80.7%.

Ultimately, the success of a survey design is dependent on the fulfillment of the user requirements. Surveys 1 and 2 will detect fewer unique objects, but the telescope slewing requirement is very small and implementation will not require a sophisticated telescope system. On the other hand, if the user requirement is to maximize the number of object observations, Survey 3 does the best job in that aspect. However, Survey 6 detects the most unique objects in both winter and summer, and is the best survey if the requirement is to maximize the number of unique object detected.

One of the important aspects of space situational awareness is to improve the state information of detected RSOs. Future work includes developing a performance metric to score the state information of the designed surveys. A performance metric such as this will be important to users with a requirement to design a survey that will maximize the total state information. Future work also includes validating all survey results using USU-STAR.

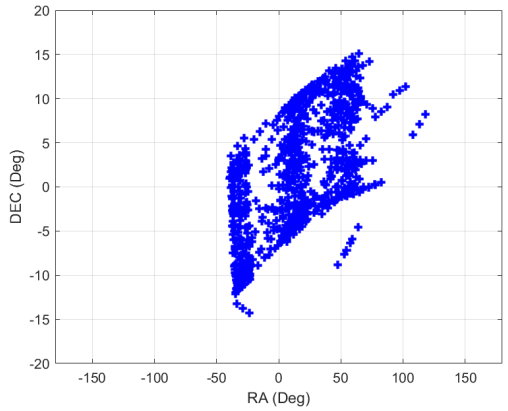

(a) Survey in geocentric right ascension and declination frame

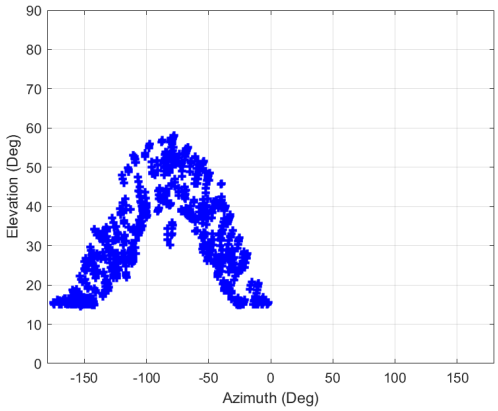

(b) Survey in geocentric azimuth and elevation frame

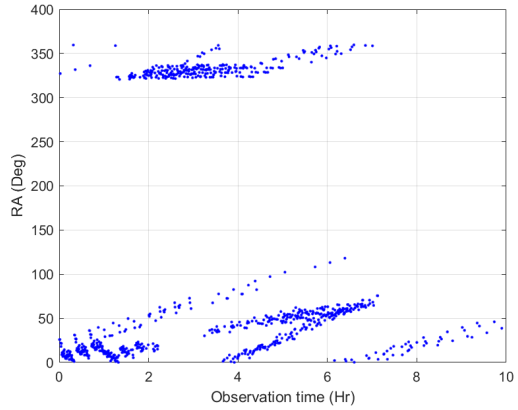

(c) RA time history

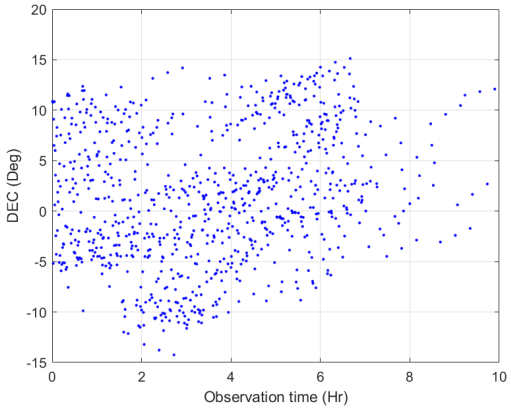

(d) DEC time history

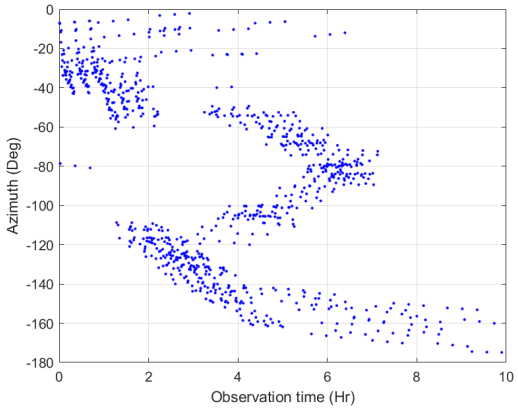

(e) Azimuth time history

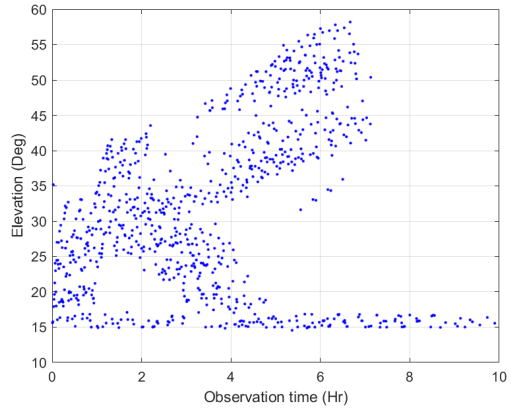

(f) Elevation time history

Fig. 11: Telescope pointing, Survey 7W (Winter, 11 Nov 2017)

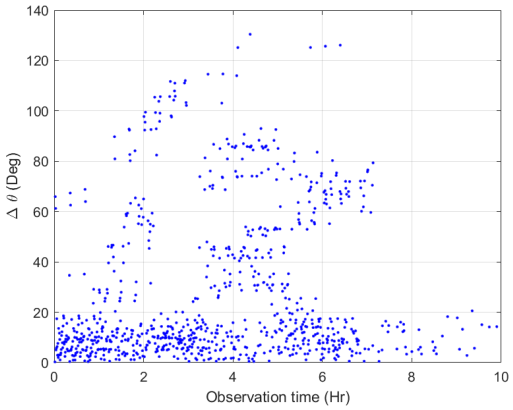

(a) $\Delta\theta$ time history

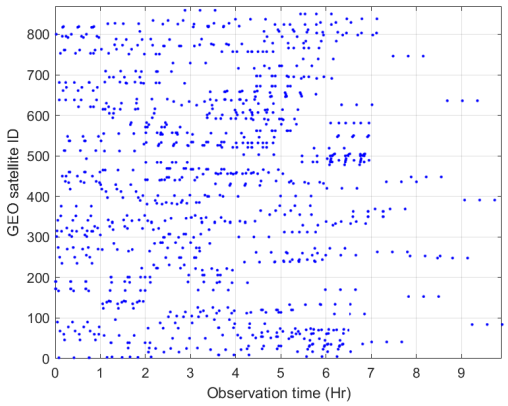

(b) GEO satellites detection time history

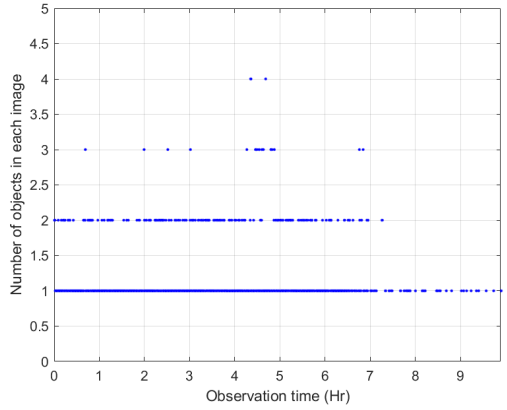

(c) Number of satellites in each image

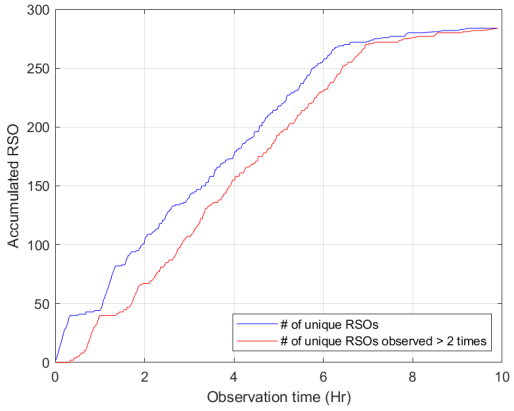

(d) Accumulation of RSO time history

Fig. 12: RSO data, Survey 7W (Winter, 11 Nov 2017)

Survey ID	# of RSO Observations	# of Unique RSOs Observed	# of Unique RSOs Observed > 2 times	Mean $\Delta\theta$ $\mu_{\Delta\theta}$(Deg)	$\mu_{\Delta\theta} + 2\,\sigma_{\Delta\theta}$ (Deg)
Survey 1W - (PPT)	917	64	64	0.07	0.08
Survey 2W - (MPPT)	801	83	80	0.19	3.07
Survey 3W - (MOO)	3833	206	158	22.91	77.42
Survey 4W - (RRDS)	1467	282	234	36.86	89.01
Survey 5W - (WOO)	2908	294	293	26.55	88.24
Survey 6W - (ROTS)	3219	295	294	35.84	93.97
Survey 7W - (GIOD)	1053	284	284	27.21	85.81

Table 2: Survey Summary (Winter, 11 Nov 2017)

Survey ID	# of RSO Observations	# of Unique RSOs Observed	# of Unique RSOs Observed > 2 times	Mean $\Delta\theta$ $\mu_{\Delta\theta}$(Deg)	$\mu_{\Delta\theta} + 2\,\sigma_{\Delta\theta}$ (Deg)
Survey 1S - (PPT)	297	21	21	0.08	0.09
Survey 2S - (MPPT)	429	37	34	0.36	6.07
Survey 3S - (MOO)	1742	126	95	23.69	79.25
Survey 4S - (RRDS)	668	215	125	37.98	90.36
Survey 5S - (WOO)	1199	233	219	31.98	92
Survey 6S - (ROTS)	1235	239	230	38.52	91.80
Survey 7S - (GIOD)	713	201	195	35.18	90.54

Table 3: Survey Summary (Summer, 17 July 2018)

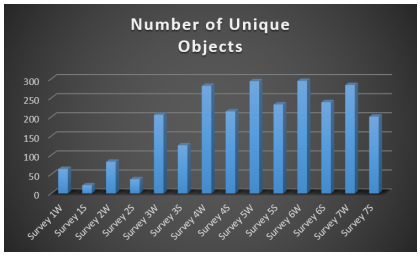

(a) Number of unique RSOs

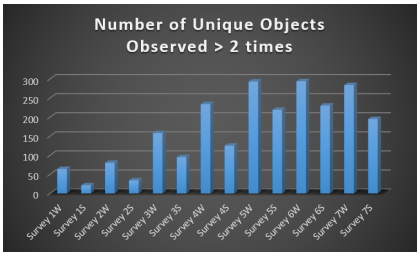

(b) Number of unique RSOs detected at least three times

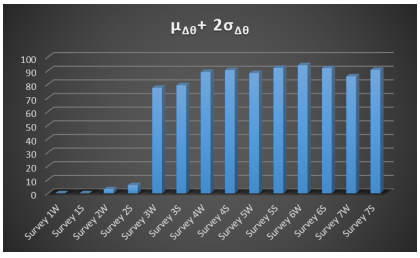

(c) $\Delta\theta$ mean plus 2σ

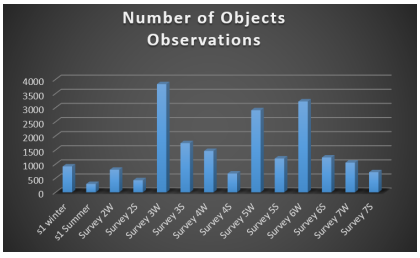

(d) Total number of objects observation

Fig. 13: Survey summary

REFERENCES

[1] John Africano, Thomas Schildknecht, Mark Matney, Paul Kervin, Eugene Stansbery, and Walter Flury. A geosynchronous orbit search strategy. *Space Debris*, 2(4):357–369, 2000.

[2] Arun J. Bernard, Akhter Mahmud Nafi, and David Geller. Using triangulation in optical orbit determination. In *AAS/AIAA Astrodynamics Specialist Conference*, 2018, AAS 18-391.

[3] T Flohrer, T Schildknecht, R Musci, and E Stöveken. Performance estimation for geo space surveillance. *Advances in Space Research*, 35(7):1226–1235, 2005.

[4] W Flury, A Massart, T Tchildknecht, U Hugentobler, J Kuusela, and Z Sodnik. Searching for small debris in the geostationary ring. *ESA bulletin*, 104:92–100, 2000.

[5] Carolin Frueh, Hauke Fielder, and Johannes Herzog. Heuristic and optimized sensor tasking observation strategies with exemplification for geosynchronous objects. *Journal of Guidance, Control, and Dynamics*, pages 1–13, 2017.

[6] Akhter Nafi, Arun Bernard, and Kohei Fujimoto. A unified approach for optical survey strategy design of resident space objects. In *AIAA/AAS Astrodynamics Specialist Conference*, page 5500, 2016.

[7] Akhter Mahmud Nafi and David Geller. Practical survey strategies for geo from a single ground based observatory. In *AAS/AIAA Astrodynamics Specialist Conference*, 2018, AAS 18-338.

[8] Alexis Petit, Daniel Casanova, Morgane Dumont, and Anne Lemaître. Creation of a synthetic population of space debris to reduce discrepancies between simulation and observations. *Celestial Mechanics and Dynamical Astronomy*, 130(12):79, 2018.

[9] T Schildknecht, R Musci, M Ploner, S Preisig, J de Leon Cruz, and H Krag. Optical observation of space debris in the geostationary ring. In *Space Debris*, volume 473, pages 89–93, 2001.

[10] T Schildknecht, M Ploner, and U Hugentobler. The search for debris in geo. *Advances in Space Research*, 28(9):1291–1299, 2001.

[11] Thomas Schildknecht, U Hugentobler, and M Ploner. Optical surveys of space debris in geo. *Advances in Space Research*, 23(1):45–54, 1999.

[12] Jayant Sharma, Grant H Stokes, Curt von Braun, George Zollinger, and Andrew J Wiseman. Toward operational space-based space surveillance. *Lincoln Laboratory Journal*, 13(2):309–334, 2002.

[13] D Talent, A Potter, and K Henize. A search for debris in geo. In *Second European Conference on Space Debris*, volume 393, page 99, 1997.

[14] SH Vaughan and TL Mullikin. Long term behavior of inactive satellites and debris near geosynchronous orbits. *Spaceflight mechanics 1995*, pages 1571–1585, 1995.